5.2.6.2 Titania vs. Alumina

The significance of titania vs. alumina support in ruthenium catalyst performance was investigated by comparing the performance of Catalysts 5245-61 and 4966-72 prepared by conventional aqueous impregnation with the same ruthenium compound on titania and alumina. Identical preparation procedures were used, except for the reduction step which was higher temperature with Catalyst 5345-61 (Table 5-42). According to STEM examination both catalysts consisted of ruthenium particles which were smaller than 2 nm. These two catalysts were tested at $2H_2$:CO feed ratio, 208°C at inlet and 35 atm in Runs 30 and 25, respectively. It was previously reported ruthenium agglomerated on alumina but was stable on titania.

Titania-supported catalyst showed 45% CO conversion at 460 gas hourly space velocity at 2 hours on stream in Run 30, while the CO conversion was 15% at 140 hr^{-1} after 2 hours on stream in Run 25 with the alumina-supported catalyst. T. initial activities in moles CO converted/sec-mol ruthenium were 0.0099 for titania-supported catalyst and 0.0028 for alumina-supported catalyst.

The selectivities of these two catalysts were compared at 11% $CO+H_2$ conversion. Selectivities to methane were similar with the two catalysts while the selectivity to C_2-C_4 products was much higher with the titania-supported catalyst. The olefin to paraffin ratios were much lower with the titania-supported catalyst which showed minimal water gas shift activity. The alumina-supported catalyst, on the other hand, apparently showed significant water gas shift activity, as previously described.

5.2.7 Selection of the Most Suitable Catalyst Development Approach

The ruthenium catalyst test results presented in Sections 5.2.1 and 5.2.2 and summarized in Section 5.2.4 indicated that a non-Anderson-Schulz-Flory catalyst approach with cutoff at a carbon number of 20 was not feasible. The products obtained with ruthenium catalysts obeyed the Anderson-Schulz-Flory law with increasing chain growth probabilities at increasing carbon numbers. By controlling the ruthenium particle size on alumina it was possible to achieve high chain growth probabilities which resulted in very low selectivity to undesirable light hydrocarbons. Catalysts prepared on titania and on Y-zeolite resulted in higher selectivities to light hydrocarbons. None of the ruthenium catalysts that were tested were stable. Improving catalytic stability while maintaining low light ends production was identified as the most suitable catalyst developmental objective. Since the ruthenium catalysts that were tested deactivated regardless of the nature of support material new ruthenium catalyst compositions were evaluated on alumina in order to improve stability. These results are described in Section 5.3.

5.3 Modification of Alumina-Supported Ruthenium Catalyst Composition to Improve Stability

5.3.1 Iron-Modified Ruthenium Catalyst with 1% Ru

An iron-modified ruthenium Catalyst 4966-102 (1% Ru, 0.5% Fe) was prepared by the reverse micelle technique and had 2-4 nm metal particles according to STEM examination. The iron:ruthenium atomic ratio in these metal particles varied between 0.3 and 1. For this catalyst, the ruthenium particle size was 4 nm according to EXAFS.

Catalyst 4966-102 was tested in Run 44 at a H_2:CO feed ratio = 2.0 at 210°C and 35 atm (Figures 5-265 through 5-269). The gas hourly space velocity was adjusted from 500 hr^{-1} to 125 hr^{-1} and then finally 75 hr^{-1} at 11 hours on stream. A maximum CO conversion of 65% was obtained at 25 hours, after which the conversion gradually declined to 36% during the following 20 hours, which indicated that the catalyst was not stable.

The iron-modified ruthenium catalyst's performance in Run 44 was not noticeably different from the performance of the ruthenium Catalyst 4966-96-1 with mostly 3-7 nm ruthenium particles and tested in Run 24 under similar conditions, except for the higher apparent water gas shift activity exhibited by the iron-modified catalyst.

Figure 5-265. Iron-Modified Ruthenium Catalyst 4966-102; Conversions in Run 44 (H_2:CO Feed Ratio = 2.0, 210°C at Inlet, 35 atm)

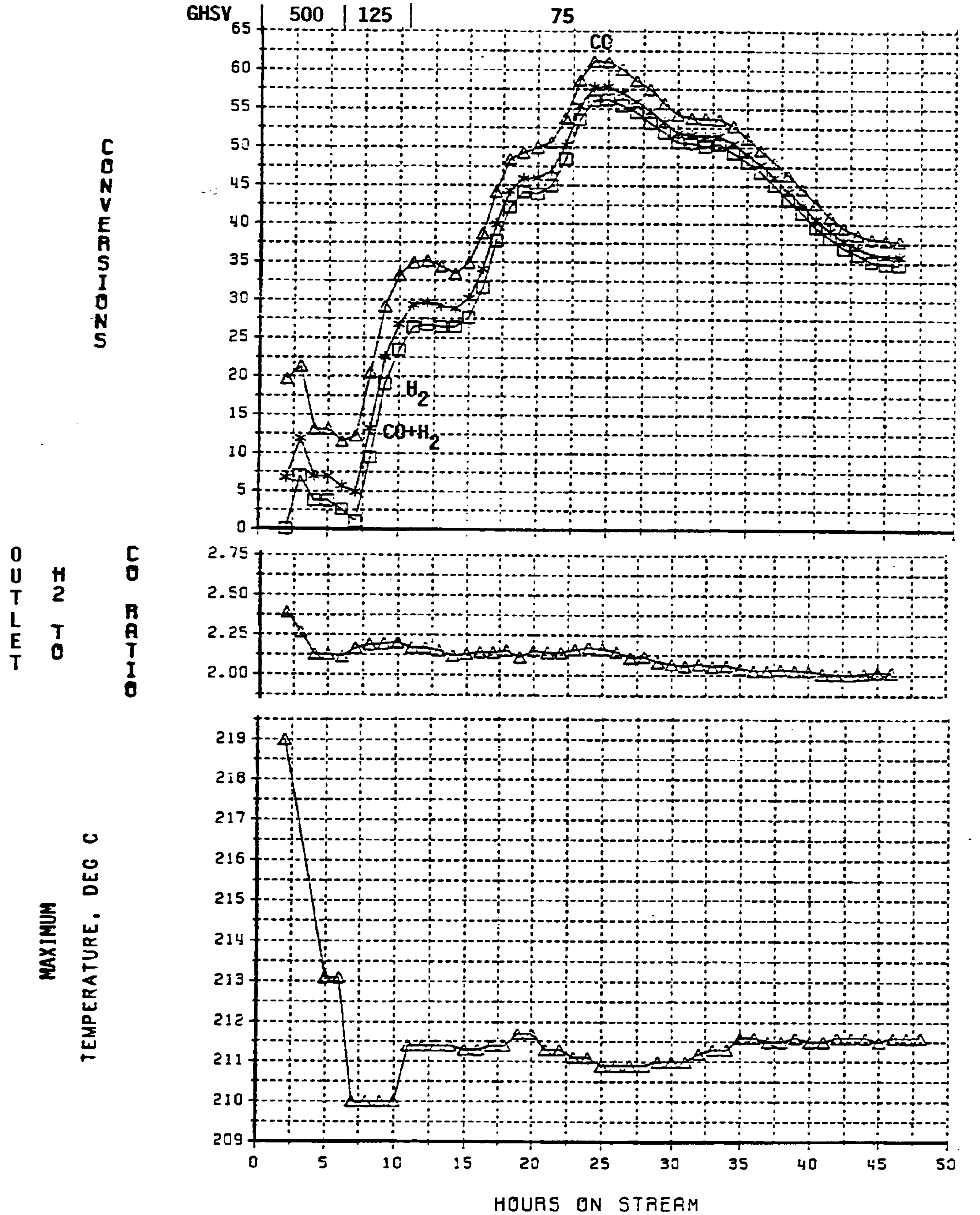

Figure 5-266. Iron-Modified Ruthenium Catalyst 4966-102: Water Gas Shift Activity in Run 44 (H_2:CO Feed Ratio = 2.0, 210°C at Inlet, 35 atm)

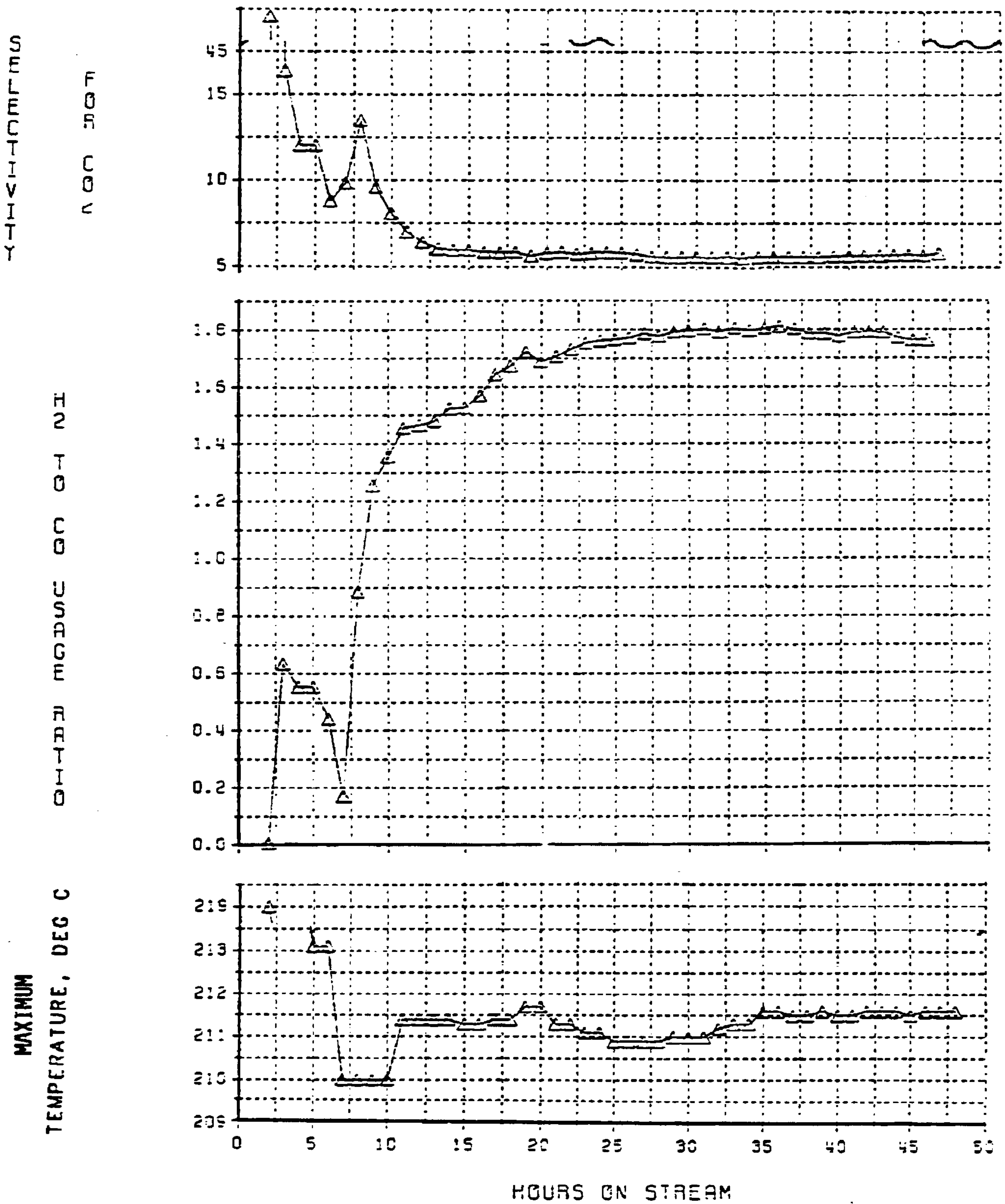

Figure 5-267. Iron-Modified Ruthenium Catalyst 4966-102: C_1 and C_2 Selectivities in Run 44 (H_2:CO Feed Ratio = 2.0, 210°C at Inlet, 35 atm)

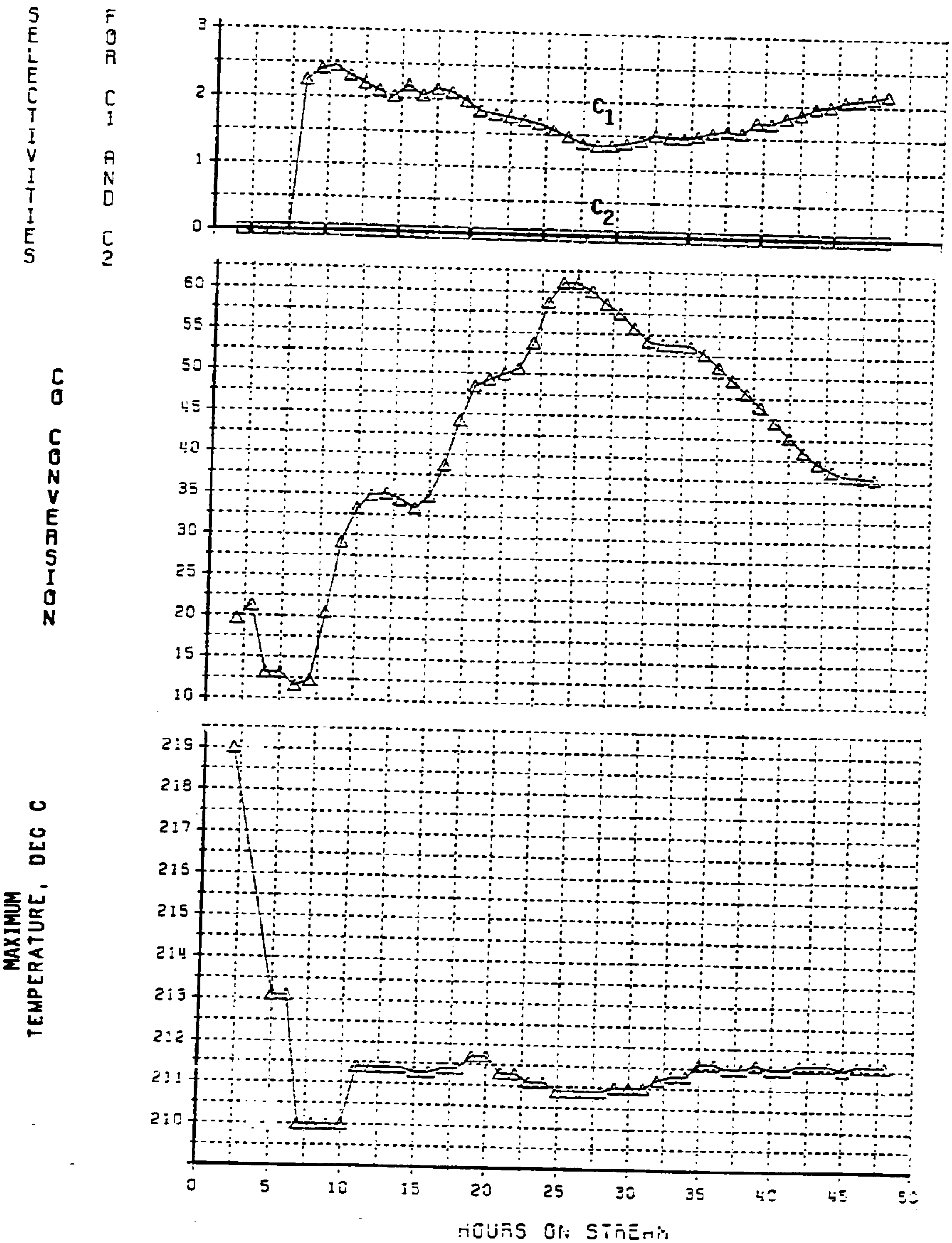

Figure 5-268. Light Hydrocarbon Selectivities in Run 44 with Iron-Modified Ruthenium Catalyst 4966-102 (H_2:CO Feed Ratio = 2.0, 210°C at Inlet, 35 atm)

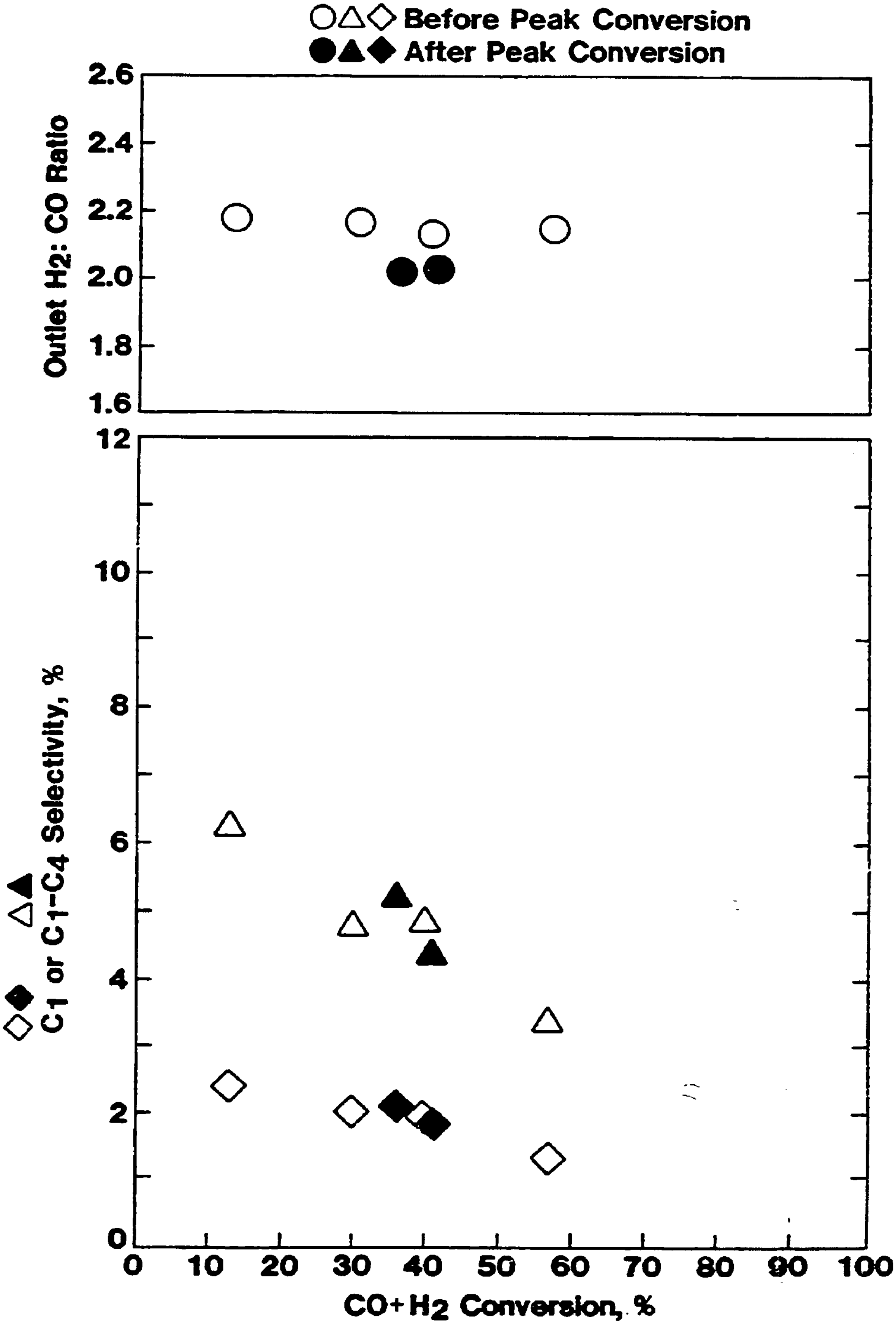

Figure 5-269. Iron-Modified Ruthenium Catalyst 4966-102:Propylene:Propane Ratios in Run 44 (H_2:CO Feed Ratio = 2.0, 210°C at Inlet, 35 atm)

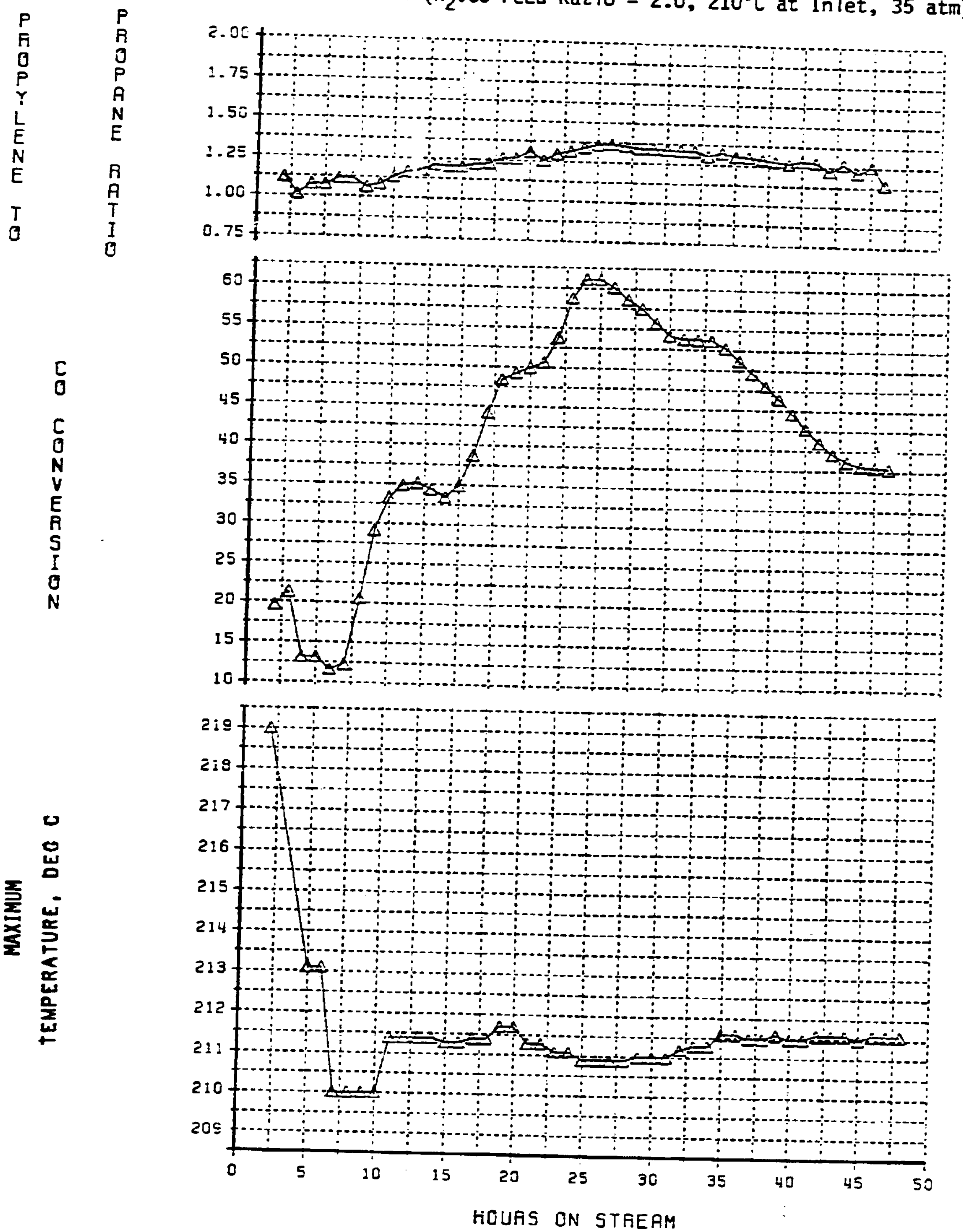

5.3.2 Ruthenium Catalyst with 2.8% Ru

Alumina-supported ruthenium catalysts with about 1% Ru were not stable. In an attempt to improve catalytic stability the ruthenium level in Catalyst 4966-198 was increased to 2.8% Ru.

Catalyst 4966-198 had a narrow size distribution of ruthenium particles in the 4-6 nm size range. This catalyst was tested in Run 47 at an inlet temperature of 208°C, 62 atm with a $2H_2$:1CO feed gas at a CO conversion level of about 75-85% in a fixed-bed reactor for 825 hours (Figures 5-270 through 5-277). This catalyst was not stable and accordingly, the gas hourly space velocity was gradually lowered from an initial value of 500 hr^{-1} to 147 hr^{-1} during the first 530 hours on stream inorder to maintain 75-85% CO conversion. After 530 hours no further space velocity change was made. The inlet temperature was increased to 210°C between 700 hours and 825 hours on stream. The CO conversion was about 72% at the end of the test (Figure 5-270).

During Run 47, once in 2-3 days, the hydrocarbon and aqueous phase products were recovered from the heated receiver. During the short period of time when products were being recovered the alternate product collection system was used. Analyses at the end of the run by GC and GPC of some of these product samples indicated that the hydrocarbon product composition did not significantly change with time on stream. Accordingly, analyses were conducted on every other sample rather than on the whole set in order to reduce analytical costs.

The hydrocarbon products collected in the heated receiver were mostly C_{10}+ and amounted to about 75% of the liquid and solid products made during the run. Lesser quantities of lighter hydrocarbon products were collected in the cooled receivers. These products were removed from the receivers less frequently.

The liquid products that accumulated inside the catalyst pores were recovered as wax by soxhlet extraction with cyclohexane.

Figure 5-270. Unmodified Ruthenium Catalyst 4966-198: CO Conversion in Run 47 (H_2:CO Feed Ratio = 2, 62 atm)

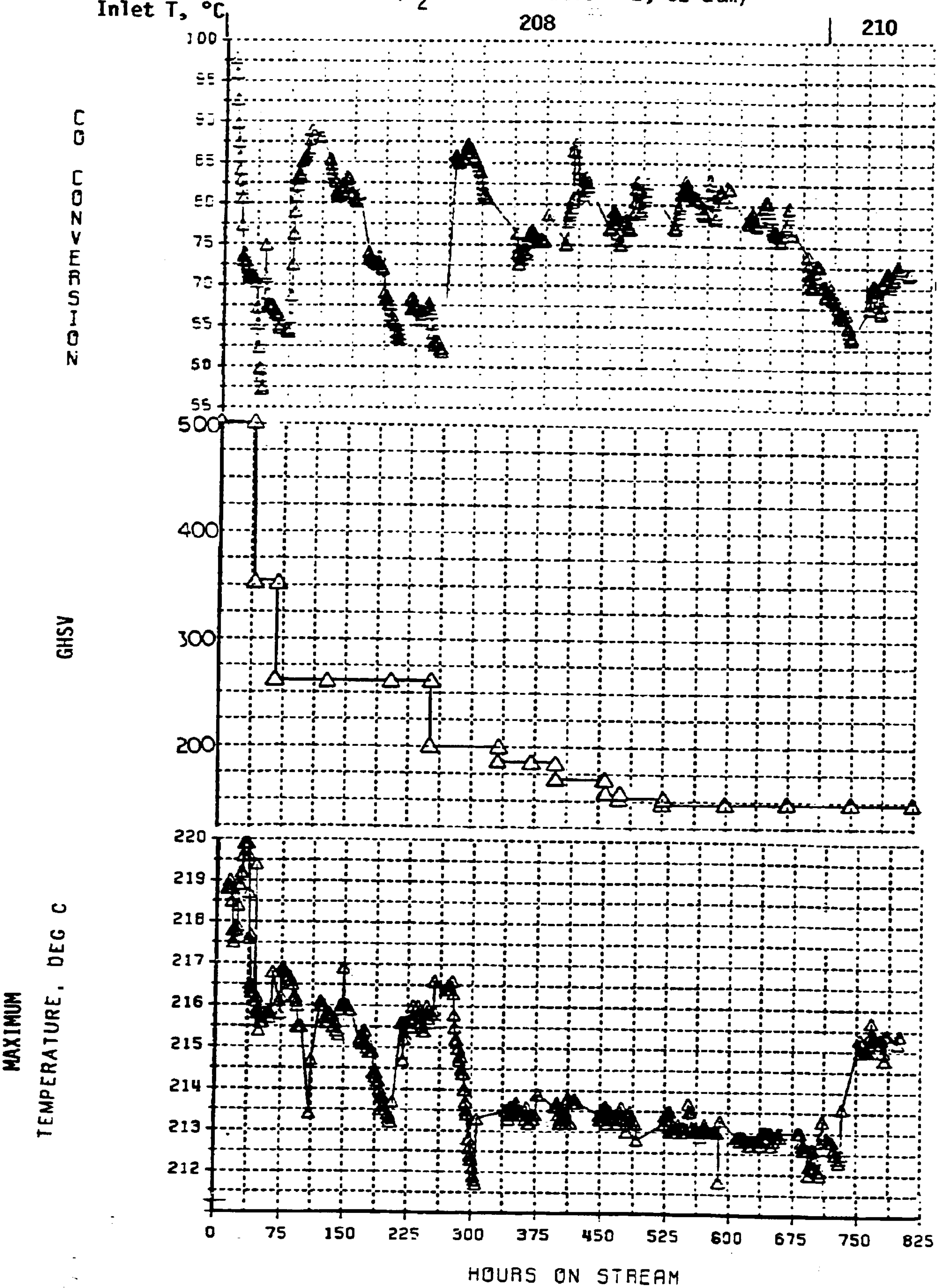

Figure 5-271. Unmodified Ruthenium Catalyst 4966-198: Water Gas Shift Activity in Run 47 (H_2:CO Feed Ratio = 2, 62 atm)

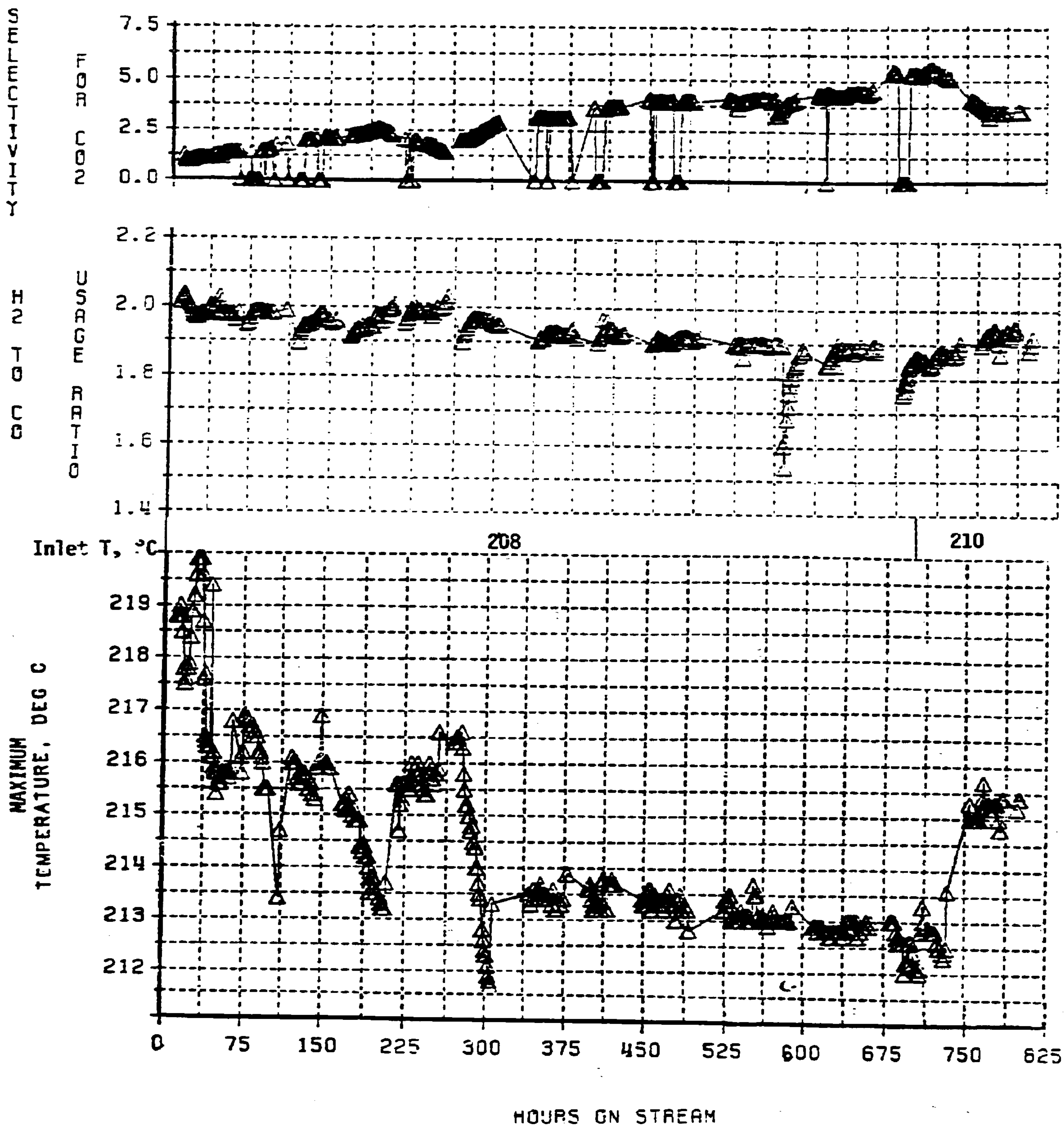

Figure 5-272. Unmodified Ruthenium Catalyst 4966-198: C_1 and C_2 Selectivities in Run 47 (H_2:CO Feed Ratio = 2, 62 atm)

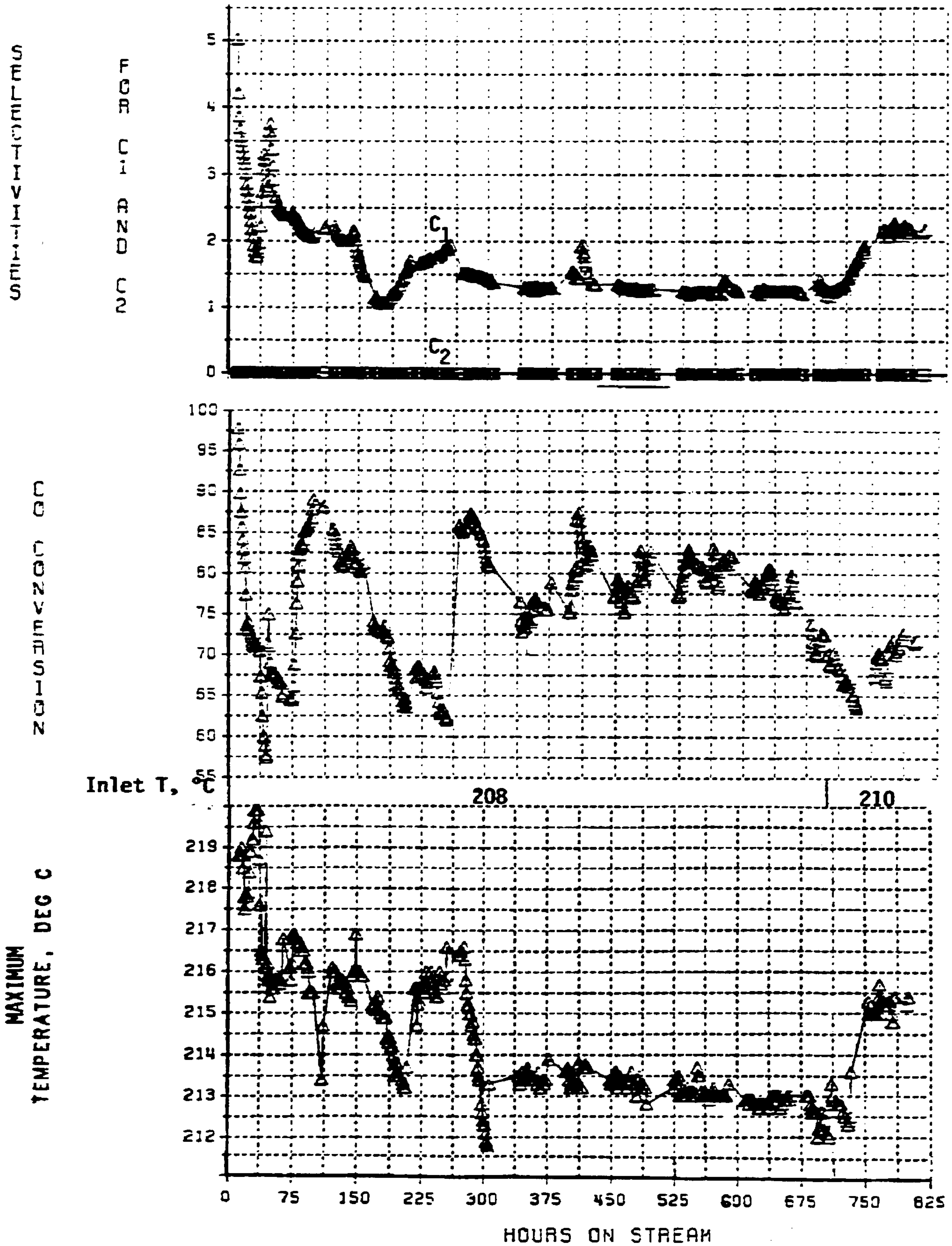

Figure 5-273. Unmodified Ruthenium Catalyst 4966-198: C_3 and C_4 Selectivities in Run 47 (H_2:CO Feed Ratio = 2, 62 atm)

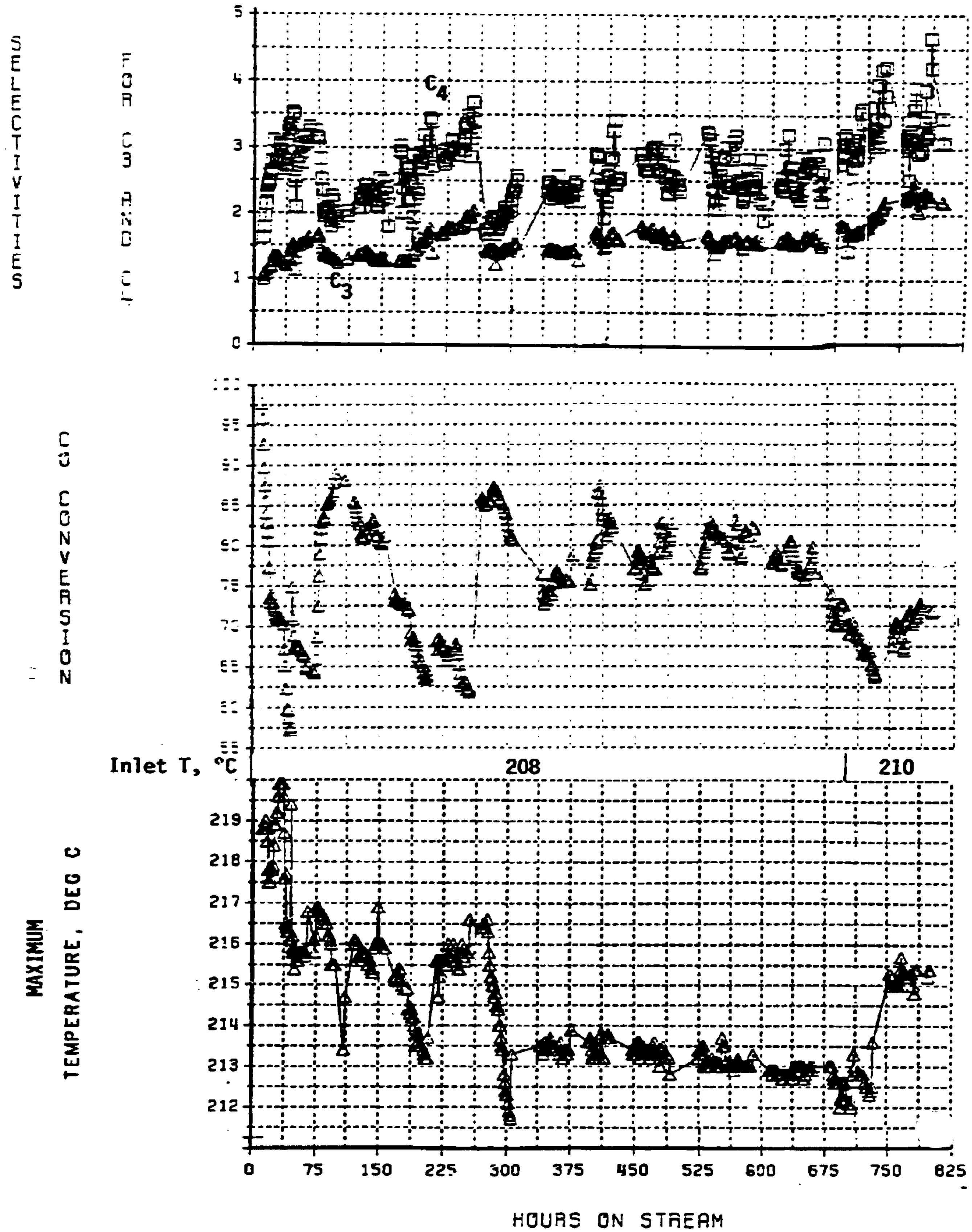

Figure 5-274. Unmodified Ruthenium Catalyst 4966-198: Propylene:Propane Ratios in Run 47 (H_2:CO Feed Ratio = 2, 62 atm)

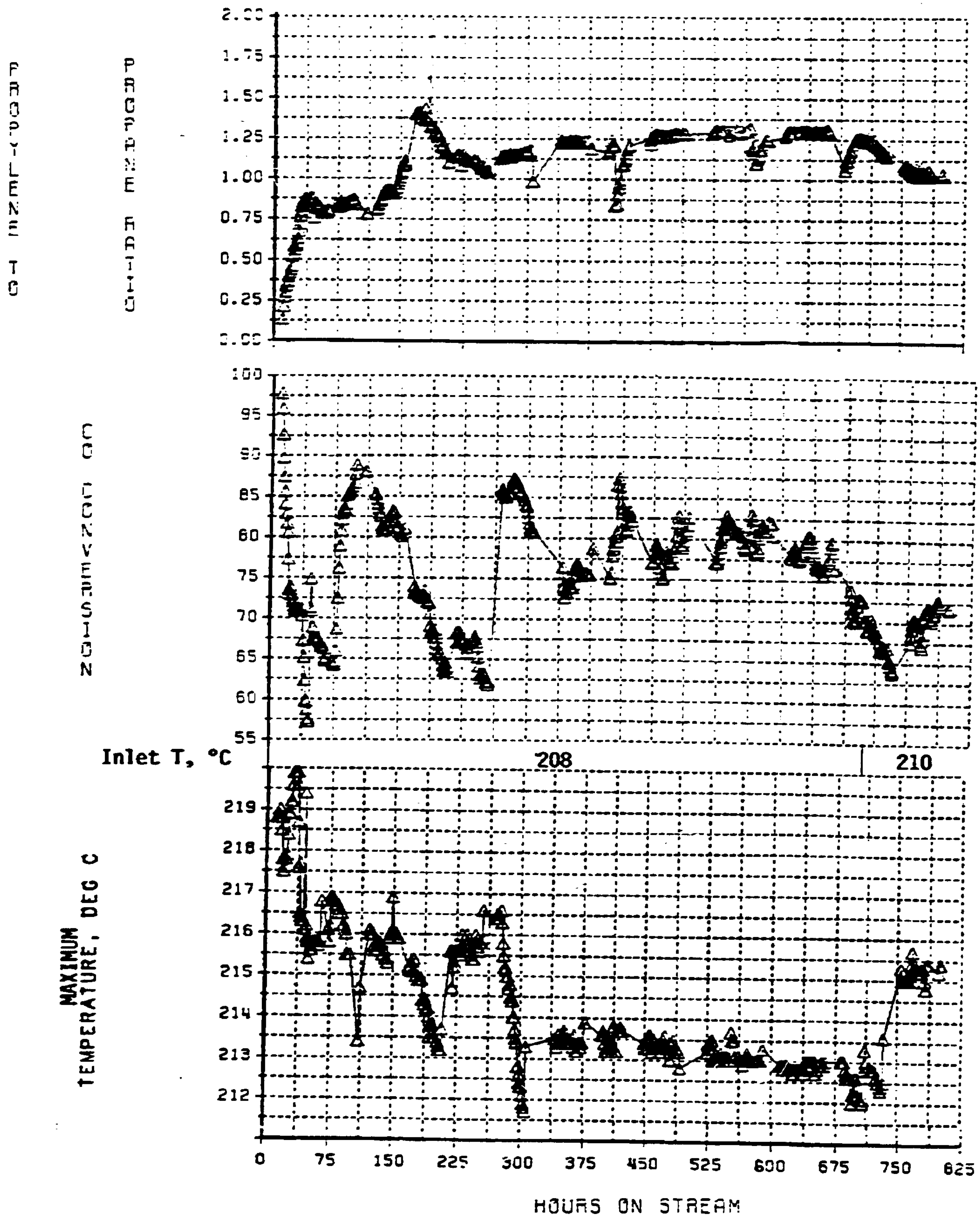

A total of 10 samples were analyzed from the 34-day-run. The overall product and the hydrocarbon distributions in Run 47 are summarized in Tables 5-47 and 5-48. The Anderson-Schulz-Flory distributions are in Figures 5-276 and 5-277. The chain growth probabilities were 0.903 at C_{13-33}, 0.941 at C_{33}-C_{70} and 0.96 at C_{70}-C_{180}.

The Anderson-Schulz-Flory distribution in Run 47 is compared in Figure 5-277b with those obtained in Runs 37 and 15 with catalysts having similar size ruthenium particles.

The operating conditions were the same in Runs 37 and 47 except for the test duration which was shorter (16 days) in Run 37. The product distributions were similar.

Run 15 was conducted at a lower H_2:CO feed ratio of 0.9 and at a lower pressure of 35 atm. The chain growth probabilities were higher for Run 15 relative to Run 47 for the entire carbon number range.

Table 5-47: Product Distributions in Run 47

HYDROCARBON DISTRIBUTION	
C1	2.708
C2 - C4	5.338
C5 - C11	15.389
C12 - C18	21.994
C19 - C25	16.824
C26 PLUS	37.746
C1 - C44	85.110
C45 PLUS	14.890
RECOVERIES	
OVERALL	85.946
CARBON	88.022
HYDROGEN	85.805
ARGON	98.759
CORRECTED RECOVERIES	
OVERALL	87.026
CARBON	89.128
HYDROGEN	86.883

GAS ANALYSIS, WT%	
HYDROGEN	3.8474
CARBON MONOXIDE	23.8088
CARBON DIOXIDE	2.9495
METHANE	0.9080
ETHANE	0.0000
ETHYLENE	0.0000
PROPANE	0.3128
PROPYLENE	0.2912
BUTANE	0.6668
BUTENE	0.3684
AQUEOUS ANALYSIS, WT%	
WATER	35.1848
ALCOHOLS	
C1	0.0413
C2	0.1112
C3	0.0097
C4	0.1123
C5	0.1305
C6	0.0773
C7	0.0531
C8	0.0340
C9	0.0212
C10	0.0106
ALDEHYDES	
C1	0.0000
C2	0.0000
C3	0.0068
C4	0.0149
C5	0.0212
C6	0.0123
C7	0.0085
C8	0.0042
C9	0.0042
C10	0.0042
OTHER OXYGENATES	
C1	0.0000
C2	0.0000
C3	0.0000
C4	0.0000
C5	0.0000
C6	0.0000
C7	0.0000
C8	0.0000
C9	0.0000
C10	0.0000

Table 5-48: Hydrocarbon Distributions in Run 47

C1	2.7079	C51	0.4583	C101	0.0643	C151	0.0119	C201	0.0034
C2	0.0000	C52	0.4371	C102	0.0621	C152	0.0116	C202	0.0031
C3	1.8492	C53	0.4173	C103	0.0600	C153	0.0112	C203	0.0030
C4	3.4886	C54	0.3983	C104	0.0578	C154	0.0109	C204	0.0029
C5	3.2838	C55	0.3796	C105	0.0558	C155	0.0096	C205	0.0029
C6	2.1651	C56	0.3623	C106	0.0528	C156	0.0094	C206	0.0028
C7	2.0452	C57	0.3455	C107	0.0509	C157	0.0092	C207	0.0027
C8	1.7573	C58	0.3299	C108	0.0491	C158	0.0089	C208	0.0027
C9	1.7948	C59	0.3151	C109	0.0474	C159	0.0087	C209	0.0026
C10	2.0058	C60	0.3019	C110	0.0457	C160	0.0085	C210	0.0026
C11	2.3375	C61	0.2893	C111	0.0441	C161	0.0083	C211	0.0024
C12	2.7015	C62	0.2776	C112	0.0425	C162	0.0081	C212	0.0024
C13	3.0327	C63	0.2667	C113	0.0410	C163	0.0078	C213	0.0023
C14	3.3207	C64	0.2573	C114	0.0395	C164	0.0076	C214	0.0022
C15	3.4208	C65	0.2474	C115	0.0381	C165	0.0075	C215	0.0021
C16	3.3448	C66	0.2375	C116	0.0368	C166	0.0073	C216	0.0020
C17	3.1651	C67	0.2278	C117	0.0355	C167	0.0071	C217	0.0020
C18	3.0088	C68	0.2183	C118	0.0343	C168	0.0069	C218	0.0019
C19	2.8140	C69	0.2090	C119	0.0331	C169	0.0067	C219	0.0018
C20	2.6597	C70	0.2001	C120	0.0320	C170	0.0065	C220	0.0017
C21	2.5389	C71	0.1916	C121	0.0310	C171	0.0064	C221	0.0017
C22	2.3965	C72	0.1836	C122	0.0299	C172	0.0062	C222	0.0016
C23	2.2662	C73	0.1756	C123	0.0290	C173	0.0060	C223	0.0015
C24	2.1404	C74	0.1690	C124	0.0281	C174	0.0059	C224	0.0015
C25	2.0084	C75	0.1628	C125	0.0272	C175	0.0057	C225	0.0014
C26	1.8962	C76	0.1571	C126	0.0263	C176	0.0056	C226	0.0013
C27	1.7880	C77	0.1517	C127	0.0255	C177	0.0054	C227	0.0013
C28	1.6827	C78	0.1465	C128	0.0248	C178	0.0053	C228	0.0012
C29	1.5922	C79	0.1416	C129	0.0240	C179	0.0052	C229	0.0012
C30	1.5009	C80	0.1366	C130	0.0233	C180	0.0051	C230	0.0011
C31	1.4221	C81	0.1317	C131	0.0227	C181	0.0050	C231	0.0011
C32	1.3322	C82	0.1267	C132	0.0220	C182	0.0049	C232	0.0011
C33	1.2487	C83	0.1218	C133	0.0214	C183	0.0048	C233	0.0011
C34	1.1991	C84	0.1173	C134	0.0208	C184	0.0047	C234	0.0010
C35	1.1233	C85	0.1126	C135	0.0202	C185	0.0046	C235	0.0010
C36	1.0890	C86	0.1081	C136	0.0196	C186	0.0045	C236	0.0010
C37	1.0239	C87	0.1039	C137	0.0190	C187	0.0044	C237	0.0010
C38	0.9900	C88	0.0999	C138	0.0184	C188	0.0043	C238	0.0010
C39	0.9301	C89	0.0962	C139	0.0179	C189	0.0042	C239	0.0010
C40	0.8668	C90	0.0928	C140	0.0168	C190	0.0042	C240	0.0010
C41	0.8479	C91	0.0896	C141	0.0163	C191	0.0041	C241	0.0009
C42	0.8099	C92	0.0866	C142	0.0158	C192	0.0040	C242	0.0009
C43	0.7657	C93	0.0838	C143	0.0153	C193	0.0040	C243	0.0009
C44	0.7497	C94	0.0812	C144	0.0148	C194	0.0039	C244	0.0009
C45	0.6182	C95	0.0786	C145	0.0143	C195	0.0038	C245	0.0009
C46	0.5874	C96	0.0761	C146	0.0139	C196	0.0038	C246	0.0009
C47	0.5586	C97	0.0736	C147	0.0134	C197	0.0037	C247	0.0009
C48	0.5312	C98	0.0712	C148	0.0130	C198	0.0036	C248	0.0009
C49	0.5051	C99	0.0689	C149	0.0126	C199	0.0036	C249	0.0009
C50	0.4809	C100	0.0666	C150	0.0123	0200	0.0035	C250	0.0009

Figure 5-275. Anderson-Schulz-Flory Distribution with Unmodified Ruthenium Catalyst 4966-198 in Run 47 (C_1-C_{44})

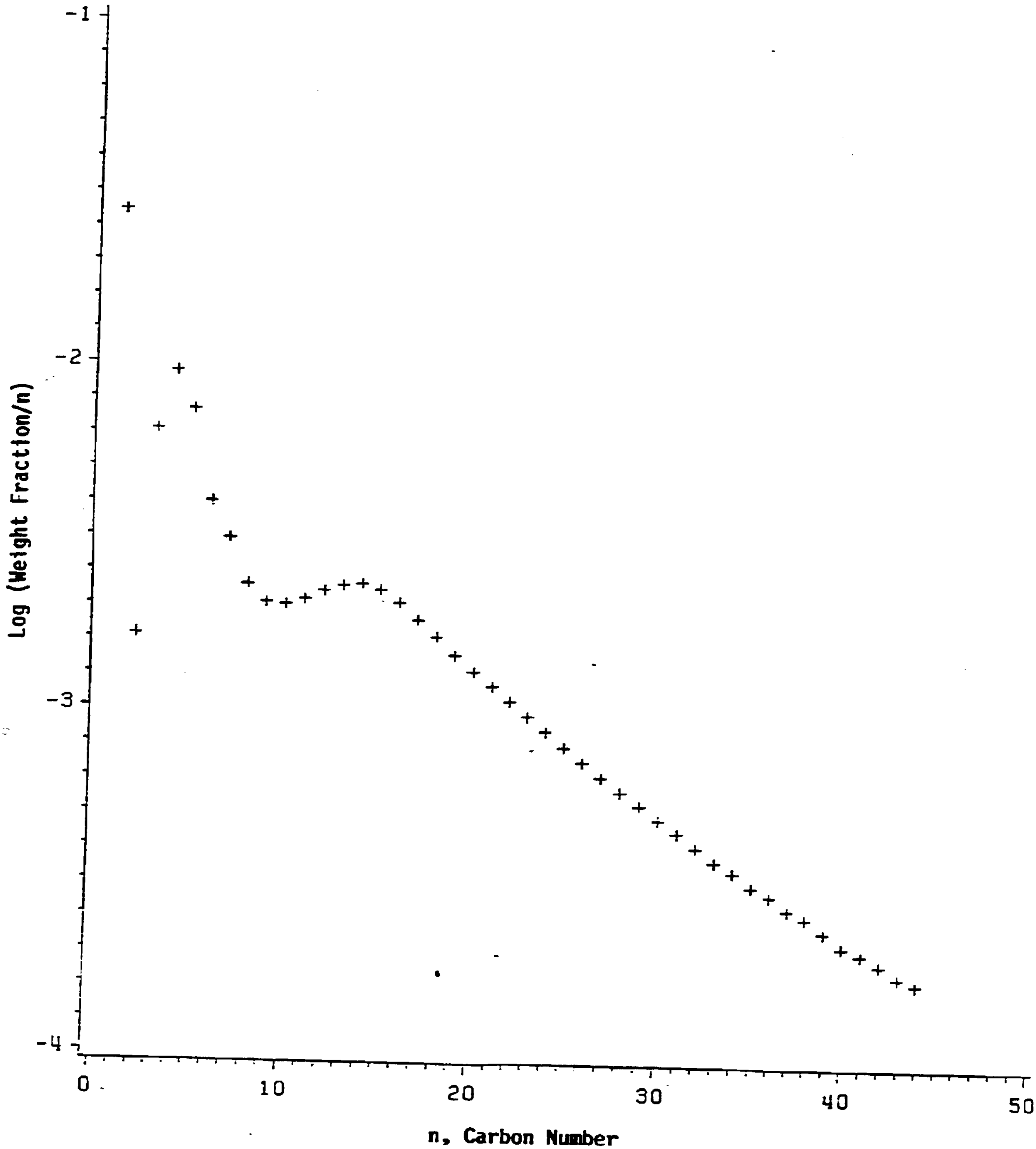

Figure 5-276. Anderson-Schulz-Flory Distribution with Unmodified Ruthenium Catalyst 4966-198 in Run 47 (C_1-C_{250})

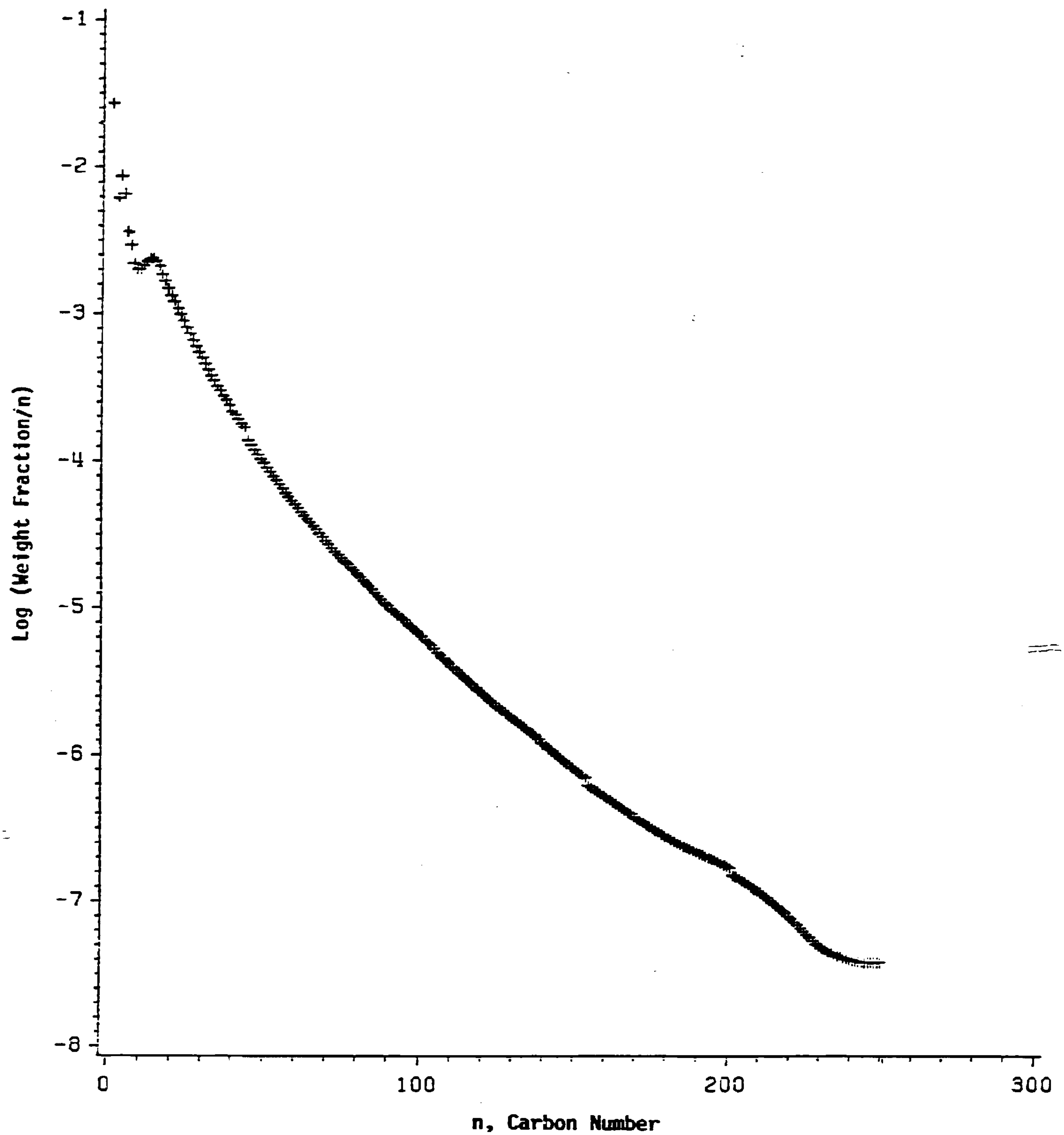

Figure 5-277. Anderson-Schulz-Flory Distributions in Runs 47, 37 and 15